Poly(methyl methacrylate) and Polystyrene/Clay Nanocomposites Prepared by in-Situ Polymerization

Changchun Zeng and L. James Lee*

Department of Chemical Engineering, The Ohio State University, Columbus, Ohio 43210

Received January 12, 2001; Revised Manuscript Received March 22, 2001

ABSTRACT: Poly(methyl methacrylate) (PMMA) and polystyrene (PS)/clay nanocomposites were prepared via in-situ bulk polymerization. The compatibility of the initiator and monomer with the clay surface was found to profoundly affect the clay dispersion. By using a surfactant containing a polymerizable group to modify the clay surface, exfoliated PMMA and PS/clay nanocomposites were synthesized. The clay dispersion was quantified by both X-ray diffraction (XRD) and transmission electron microscopy (TEM). The dimension stability of nanocomposites was studied and related to both nanoscale (layer separation) and mesoscale (long-range distribution) clay dispersion.

Introduction

Since Toyota's pioneering work on polymer layered silicate nanocomposites,[1−3] a great deal of research has been carried out in this field over the past decade. With the addition of a very small amount of nanofiller into the polymer matrix, these nanocomposites exhibit substantial increase in many physical properties, including mechanical properties (tensile modulus and strength, flexural modulus, and strength), [3−8] thermal stability,[3,8,9] flame retardance,[10−13] and barrier resistance.[3,8,14−16] Smectite clays, such as montmorillonite (MMT), are of particular interest because they offer a high aspect ratio (10−1000) and a high surface area. Montmorillonite is hydrophilic in nature, which hinders the homogeneous dispersion in the organic polymer phase. Ion exchange of the interlayer inorganic cations (Na^+, Ca^{2+}) with organic cation renders the hydrophilic clay surface organophilic. The reduction in surface energy improves the wetting characteristics of the clay surface with polymers or monomers.[17,18]

From the structural point of view, two idealized polymer/clay nanocomposites are possible: intercalated and exfoliated. Intercalation results from the penetration of polymer chains into the interlayer region and interlayer expansion. Usually the ordered layer structure is preserved and can be detected by X-ray diffraction (XRD). By contrast, exfoliation involves extensive polymer penetration and silicate crystallites delamination, and the individual nanometer-thick silicate platelets are randomly dispersed in the polymer matrix. Exfoliated nanocomposites usually provide the best property enhancement due to the large aspect ratio and surface area of the clay.

Melt intercalation and in-situ polymerization are the two most common ways of preparing polymer/clay nanocomposites. Melt intercalation involves the mixing of clay with a molten polymer matrix. The layer separation, especially exfoliation, depends on the establishment of favorable interactions between the polymer and the clay surface and the subsequent system energy reduction.[19−23] In-situ polymerization involves monomer intercalation followed by polymerization. By tailoring the interaction between the monomer, the surfactant, and the clay surface, the exfoliated nanocomposites (nylon-6,[2] poly(ϵ-caprolactone),[16] and epoxy[4,9,24−26]) were successfully synthesized via ring-opening polymerization. The functional group in the organic cation can catalyze intralayer polymerization and facilitate layer separation.

Many thermoplastic polymers are produced by free radical polymerization using vinyl monomers, and the reaction adopts distinctly different mechanisms as compared to ring-opening polymerization.[27] Polymerization is usually carried out in the presence of initiators. It is therefore necessary to investigate the interaction between the monomer, the initiator, and the modified clay surface in a systematic manner. Intercalated PMMA and PS nanocomposites have been synthesized through either emulsion[28,29] or bulk polymerization.[30,31] It was found that the structural affinity between the styrene monomer and the organic cation played an important role in the PS/clay hybrid structure.[32] Improved dispersion of clay in the PMMA/clay nanocomposites was obtained when MMA was co-intercalated and copolymerized with lauryl methacrylate (LMA). The authors attribute this improvement to a better compatibility of LMA with the organic cation functionalized clay surface.[33] Efforts have also been made to anchor a living free radical polymerization (LFRP) initiator in the interlayer region to improve the intralayer polymerization rate, to achieve an exfoliated PS nanocomposite.[34] Recently, a more conventional initiator, 2,2′-azo(isobutylamidine hydrochloride), was immobilized in the interlayer region to yield exfoliation of clay in the PMMA matrix, using suspension polymerization.[35] Exfoliation of clay in PMMA was also reported in the emulsion polymerization.[36] Our work focuses on the synthesis of exfoliated PMMA and PS/clay nanocomposites via bulk polymerization. The effects of monomer, initiator, and clay surface modification on the structure of nanocomposites are investigated.

Experimental Section

Materials. Two monomers, methyl methacrylate (MMA) and styrene (St), and two initiators, benzoyl peroxide (BPO) and 2,2′-azobis(isobutyronitrile) (AIBN), were purchased from Aldrich. All materials were used as received. An organophilic clay Cloisite 20A (20A), which is a dimethyl dihydrogenated tallow ammonium montmorillonite, was provided by Southern

* To whom correspondence should be addressed.

10.1021/ma010061x CCC: $20.00
Published on Web 05/03/2001

Scheme 1. Synthesis of MHAB

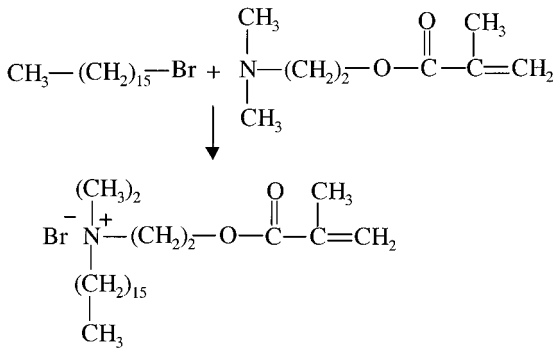

Clay. Na^+−montmorillonite (Wyoming SWy2) was purchased from the Clay Source Repository, University of Missouri, Columbia. It has an ion exchange capacity of 76.4 mequiv/100 g. A polystyrene (Styon 685D from Dow Chemical) was used to prepare the PS/clay nanocomposite by extrusion compounding.

Synthesis of Reactive Surfactant MHAB for MMT Modification. A reactive cationic surfactant 2-methacryloyloxyethylhexadecyldimethylammonium bromide (MHAB) was synthesized by the quaternarization reaction as shown in Scheme 1. 2-(Dimethylamino)ethyl methacrylate and 1-bromohexadecane (2:1 molar ratio) (Aldrich) were reacted at 60 °C for 24 h, in the presence of 3000 ppm inhibitor hydroquinone monomethyl ether (MEHQ) (Aldrich). The product is insoluble to either ingredient and thus precipitated. The white powder-like precipitant was purified by filtering and washing using ethyl acetate (Aldrich). It was then dried under vacuum at ambient temperature for 24 h.

Preparation of Organophilic Clay MHABS. An organophilic clay was prepared by the ion exchange reaction. SWy2 clay (10 g) was dispersed in 800 mL of deionized water at room temperature. MHAB (5.3 g, 0.0115 mol) was dissolved in 200 mL of deionized water and slowly poured into the clay suspension. The suspension was stirred for 24 h at room temperature. The exchange clay was then filtered using a Busch filter and redispersed in deionized water. This procedure was repeated several times until no bromide ion was detected with 0.1 N $AgNO_3$ solution. The filter cake was vacuum-dried at room temperature and crushed into powder using a mortar and pestle. The organophilic MMT is denoted as MHABS.

Preparation of Polymer/Clay Nanocomposites. The monomer/clay mixture was sonicated for 6 h before a certain amount of initiator was added. The mixture was then sonicated for another 1 h. Polymerization was carried out under isothermal conditions. The reaction time varied from 4 to 20 h, depending on the reaction temperature and the type and amount of initiator added. Prepared hybrids were then postcured in an oven at 105 °C. PS/20A nanocomposites were also prepared using a Leistritz ZSE-27 intermesh twin screw extruder (L/D = 40, d = 27 mm) operated in the corotating mode. The barrel temperature was set at 200 °C and the screw speed 90 rpm. Prepared nanocomposites were compared with in-situ polymerized nanocomposites at the same level of clay loading. All PS/clay nanocomposites were injection molded into tensile bars using a DACA microinjector with a barrel temperature of 220 °C and mold temperature of 85 °C.

Structure Analysis of Nanocomposites. The X-ray diffraction (XRD) spectra of prepared polymer/clay nanocomposites were recorded on a Scintag XDS-2000 Θ∼Θ X-ray diffractometer equipped with an intrinsic germanium detector system using Cu Kα radiation (λ = 1.5418 Å). Transmission electron microscopy (TEM) was also adopted to characterize the nanocomposites structure. Unless otherwise specified, TEM was performed on a Phillip CM200 using an accelerating voltage of 200 kV. The nanocomposite samples were sectioned into ultrathin slices (<100 nm) at room temperature using a microtome equipped with a diamond knife and then mounted on 200 mesh copper grids.

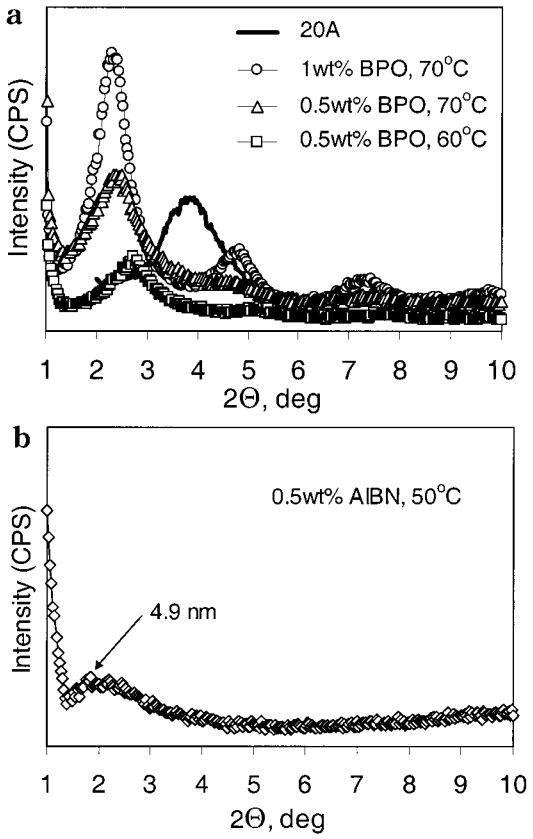

Figure 1. XRD patterns of PMMA/20A(5 wt %) nanocomposites with (a) BPO and (b) AIBN as initiator. Diffraction pattern of 20A is included as a reference.

Dimension Stability at Elevated Temperature. Portions of injection molded tensile bars were placed in an oven and heated to the following temperatures: 50, 75, 105, and 135 °C, each for 1 h, for a total of 4 h. Sample dimensions before and after the thermal cycle were imaged using a digital camera.

Results and Discussion

Effect of Initiators and Monomers. The clay 20A was used to prepare PMMA/clay nanocomposites. It has an interlayer spacing of d = 2.3 nm. Figure 1a compares the XRD spectra of the nanocomposites prepared with different amounts of BPO at two temperatures**,** and the interlayer spacing for the nanocomposites is listed in Table 1. In each case, clay content was fixed at 5 wt %, and a distinct basal reflection (d001) peak was observed, indicating that an intercalated nanocomposite was obtained. The nanocomposites prepared at 60 °C showed a slightly smaller interlayer spacing (d = 3.5 nm) than the other two (d = 3.6 nm). In the range of experimental conditions, varying the initiator amount and reaction temperature did not result in a substantial alteration of the interlayer spacing. Polymerization was also conducted at 50 °C, using AIBN as the initiator, and the XRD pattern of the prepared nanocomposite is shown in Figure 1b. Only a very weak and broad peak at d = 4.9 nm is present, indicating a highly disordered intercalated nanocomposite with greater layer separation and a reduced extent of layer stacking.[37,38] This is also supported by the TEM observation. Figure 2a is the TEM micrograph of a PMMA/20A nanocomposite prepared using BPO as the initiator. The dark lines are the clay layers perpendicular to the sample surface. Large clay aggregates (particles) are visible, although

Table 1. Summary of Interlayer Spacing of 20A and PMMA/20A Nanocomposites Shown in Figure 1a[a]

material	20A	MMA/1 wt % BPO/20A	MMA/0.5 wt %BPO/20A	MMA/0.5 wt %BPO/20A
reaction temp (°C)		70	70	60
interlayer spacing (nm)	2.3	3.6	3.6	3.5

[a] Clay loading is 5 wt % in each of the nanocomposites.

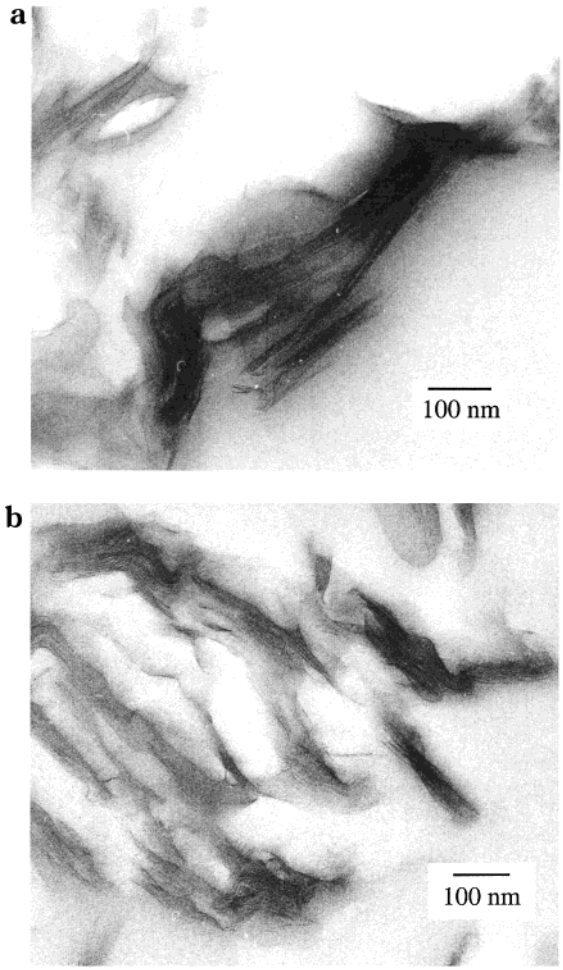

Figure 2. TEM micrographs of PMMA/20A(5 wt %) nanocomposites prepared under different reaction conditions: (a) initiator, 1 wt % BPO; temperature, 70 °C; (b) initiator, 0.5 wt % AIBN; temperature, 50 °C.

the interlayer spacing is expanded. On the other hand, the nanocomposite prepared by using AIBN as the initiator shows much better clay dispersion (Figure 2b). While the individual clay layer is visible, small aggregates can still be observed in some regions. The clay platelets are flexible and show substantial curvature in many instances.

PS/20A nanocomposites with a clay content of 5 wt % were also prepared using these two initiators, and the XRD spectra of the resulting nanocomposites are shown in Figure 3. Both nanocomposites show a diffraction peak with an identical interlayer spacing of $d = 3.4$ nm. Improved dispersion of the clay in the PMMA matrix was achieved when AIBN was used. On the other hand, the basal spacing of PS/20A nanocomposites was found to be independent of the choice of initiator.

In the monomer/initiator/organophilic clay systems discussed here, the interactions of both initiator and monomer with the organophilic clay need to be considered. AIBN possesses two highly polar nitrile groups, leading to a higher polarity than BPO. The presence of two benzene rings makes BPO more hydrophobic than

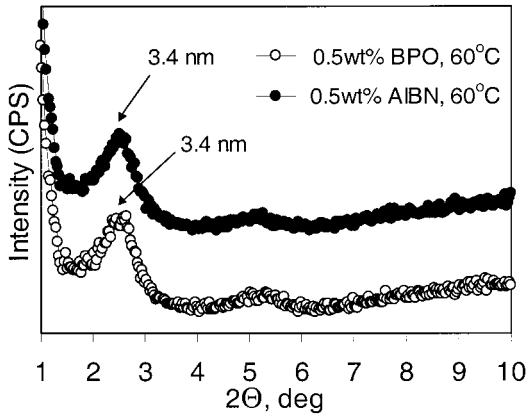

Figure 3. XRD patterns of PS/20A(5 wt %) nanocomposites. Curves are vertically offset for clarity.

AIBN. The MMT clay surface is polar and hydrophilic in nature. During the ion exchange reaction, the hydrophilic nature decreases as the organic cations replace the original inorganic cations. However, a portion of the clay surface may not be covered by the organic cation, which makes the surface-treated clay still more compatible with polar molecules.[39] As a result, the AIBN/MMA/clay system has a better clay dispersion than the BPO/MMA/clay system.

The failure to achieve better clay dispersion in PS using AIBN as the initiator implies that the compatibility of the monomer with the organophilic clay is also an important factor. MMA contains both a low polar portion (methacryl group) and a high polar portion (ester group). The polarity of MMA is higher than that of styrene, as verified by the dipole moment difference of the two (μ(MMA) = 1.7 D, μ(St) = 0.37 D).[40] Blumstein[40] and Solomon et al.[41] showed that MMA has a stronger compatibility with the polar clay surface than styrene. The organic cation in 20A contains a positively charged ammonium headgroup and a nonpolar aliphatic chain. Upon MMA intercalation, more favorable interaction between MMA and clay surface may be established due to their polar nature. In addition, the van der Waals interaction is also established between the low polar methacryl group and the nonpolar alkyl chain in the organic cations. It has been shown that media that possess both polar and nonpolar characteristics had excellent ability to swell and disperse ammonium onium modified organophilic MMT.[39,42] This is why polar additives are widely used to enhance the dispersion of organophilic clay in nonpolar hydrocarbon.[43,44]

Effect of Surface Modification. The organophilic clay MHABS was synthesized as mentioned in the Experimental Section, and the X-ray diffraction pattern is shown in Figure 4 (curve a). Compared to the basal spacing of Na^+−MMT (0.95 nm[37]), the increase of the basal spacing ($d = 1.95$ nm) clearly shows the intercalation of the reactive cation into the interlayer region. The PMMA/clay nanocomposite was prepared using 5 wt % MHABS. Polymerization was carried out at 50 °C with 0.5 wt % AIBN as the initiator. The resultant nanocomposite exhibits a featureless XRD pattern, as shown in

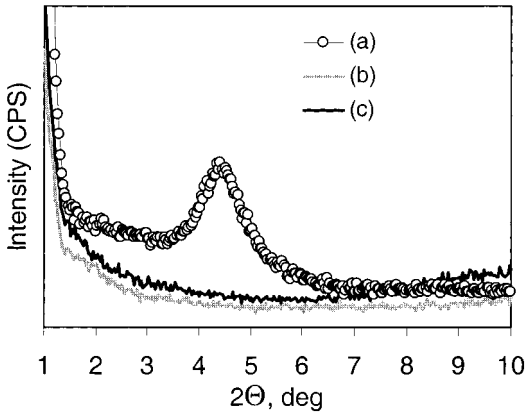

Figure 4. XRD pattern of (a) MHABS, (b) PMMA/MHABS(5 wt %), and (c) PS/MHABS(5 wt %) nancomposites. In (b) and (c), 0.5 wt % AIBN was used in preparing nanocomposites. Reaction temperatures were 50 °C for MMA/AIBN/MHABS and 60 °C for St/AIBN/MHABS.

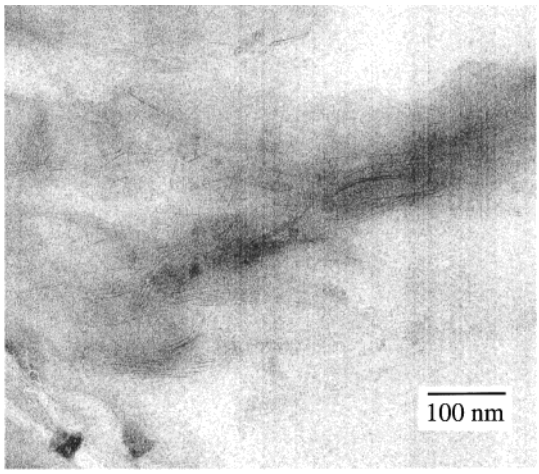

Figure 5. TEM micrograph of PMMA/MHABS(5 wt %) nanocomposite**.** Image corresponds to curve b in Figure 4.

Figure 4 (curve b), suggesting possible exfoliation. The TEM micrograph in Figure 5 clearly shows that individual clay platelets are randomly distributed in the PMMA matrix. A small amount of stacking of several layers with substantial layer separation is also visible.

The PS/MHABS (5 wt %) nanocomposite was prepared in the presence of 0.5 wt % AIBN at 60 °C. The XRD pattern of the resulting nanocomposite (Figure 4, curve c) reveals exfoliation, as verified by the absence of any diffraction peaks. This was further confirmed by TEM micrograph shown in Figure 6. All of the clay tactoids have been disrupted and uniformly distributed in the PS matrix.

In a way similar to an immobilized initiator in the interlayer region, an anchored organic surfactant with polymerizable groups may provide an additional kinetic driving force for layer separation. We suspect that copolymerization of the intercalated monomer and the organic cation may gradually push the layers apart, leading to delamination of clay tactoids. A similar route was adopted by Fu et al.[45] in preparing PS/clay nanocomposites using a surfactant containing a styryl group. In addition to the kinetic driving force, the structural similarity of the organic cation and styrene may result in a stronger interaction and lead to improved swelling of the clay.

Dimension Stability at Elevated Temperature of PS/Clay Nanocomposites. Figure 7 shows the shape changes of injection molded PS and PS/clay nanocomposites under the aforementioned thermal cycle (50 °C, 1 h; 75 °C, 1 h; 105 °C, 1 h; and 135 °C, 1 h). The original sample shape is shown in the first row. Pure PS (Styron 685D) and the extruded PS/20A nanocomposite are shown in the second row for comparison. The third row shows the in-situ polymerized pure PS, PS/20A, and PS/MHABS nanocomposites. All the nanocomposites contain 5 wt % clay. In all cases, reaction was conducted at 60 °C with 0.5 wt % AIBN. In the absence of clay, the sample shrank greatly, and the shape became highly irregular. Dimension stability at elevated temperature was improved significantly when 5 wt % of clay was present in the in-situ polymerized nanocomposites, as shown in the third row. The exfoliated PS/MHABS exhibited the best dimensional stability. After the heating cycle, although the sample shrank to a certain extent, the original shape and surface smoothness remained. It is noteworthy that the PS/20A nanocomposite prepared by extrusion compounding (in the second row of Figure 8) did not show much improvement in dimension stability at elevated temperature, as compared to the in-situ polymerized PS/20A nanocomposite with the same clay loading.

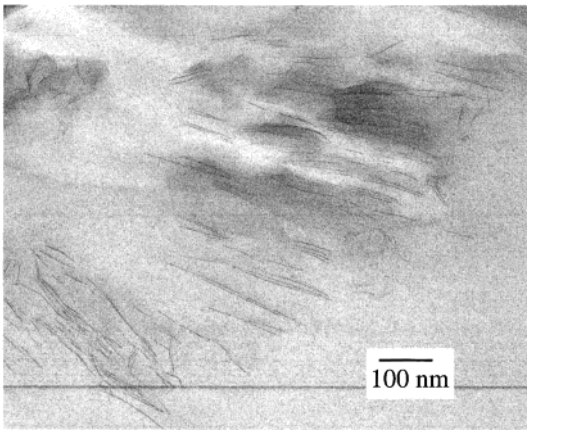

Figure 6. TEM micrograph of PS/MHABS(5 wt %). Image corresponds to curve c in Figure 4.

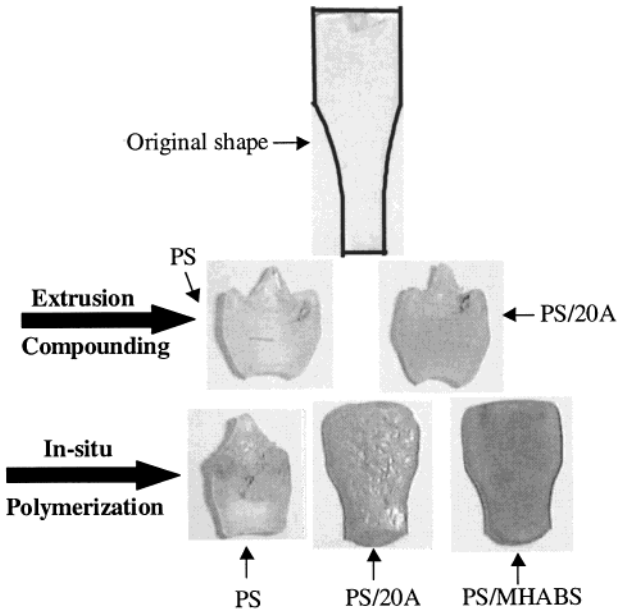

Figure 7. PS and PS/clay nanocomposites after dimension stability test. Clay loading is 5 wt % for all nanocomposites.

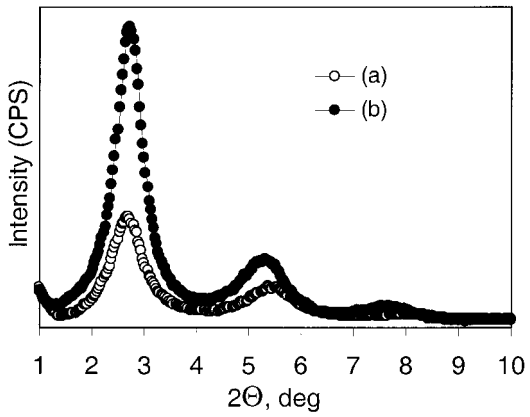

Figure 8. XRD patterns of injection molded PS/20A(5 wt %) nanocomposites by (a) extrusion compounding and (b) in-situ polymerization.

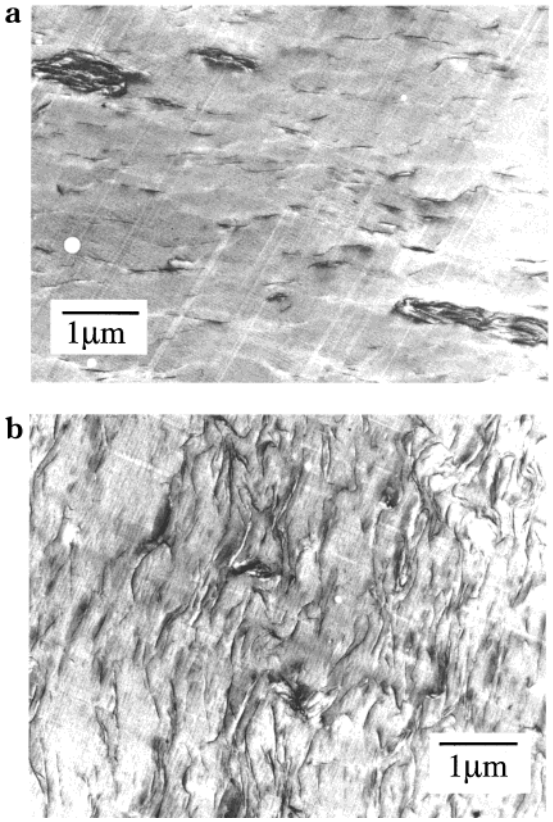

Figure 9. TEM micrographs of injection molded PS/20A(5 wt %) nanocomposites by (a) extrusion compounding and (b) in-situ polymerization. Samples were cut from the center of the tensile bars and were perpendicular to the flow direction. Images were collected using a Phillips C12 operated at 60 kV.

The X-ray diffraction spectra of the two injection molded PS/20A nanocomposites are shown in Figure 8. The basal reflections (d001) are similar. However, a substantial difference is observed in the TEM micrographs of these two nanocomposites, as shown in Figure 9. Images were recorded on Phillips C12 operated at 60 kV. In the extruded nanocomposite, large clay aggregates are observable in many places. On the other hand, the clay distribution is more uniform in the in-situ polymerized nanocomposite.

There are apparently two levels of clay dispersion and distribution in the polymer matrix. The first is nanoscale dispersion, involving layer separation of the clay. The chemical compatibility and physical interaction between the treated clay surface and intercalated species determine the degree of layer separation.[19−23] The second level, the mesoscale distribution of clay, involves the disruption of clay aggregates and primary particles.[46,47] It affects the long-range clay structure and polymer matrix−clay interaction.[48,49] It is also a time and mixing strength dependent process.[46,50] Figure 9a (TEM) shows insufficient mesoscale clay distribution in the extruded nanocomposite, possibly due to inadequate mixing. In the in-situ polymerized nanocomposites, clay particles are dispersed more uniformly (Figure 9b) on the mesoscale with the help of sonication. In fact, during sonication, the viscosity of the monomer/clay mixture kept increasing and gelation occurred. Similar results were also observed by other researchers.[9,33,45] This is an indication of network formation by the disruption and dispersion of clay aggregates.[51] Even though these two nanocomposites have a similar nanoscale dispersion as verified by XRD, the mesoscale dispersion and distribution differ. Better dispersion of clay at the mesoscale in the in-situ polymerized nanocomposite results in better reinforcement of the matrix, leading to higher dimension stability. Disruption of the clay tactoids (exfoliation) provides a large increase of effective aspect ratio and surface area, resulting in further reinforcement.

Conclusions

PMMA and PS/clay nanocomposites incorporating with organo-modified clays were prepared by in-situ polymerization. It was found that the polarity and hydrophilicity of the initiators and monomers greatly affect dispersion of the clay. The combined use of a more polar, less hydrophobic monomer and initiator leads to better clay layer separation and a more disordered intercalated nanocomposite. This is a result of the favorable interactions of the clay surface with both the monomer and the initiator. Introducing polymerizable groups onto the clay surface improved the clay dispersion significantly, and exfoliated PMMA and PS/clay nanocomposites were successfully synthesized with a clay concentration of 5 wt %. The presence of clay can substantially improve the dimension stability of the polymer matrix in an exfoliated nanocomposite with uniform mesoscale clay dispersion.

Acknowledgment. This work was supported by National Science Foundation funded Center for Advanced Polymer and Composite Engineering (CAPCE) at The Ohio State University. The authors thank Southern Clay and Dow Chemical for material donation. We also acknowledge Kathy Wolken, Hendrik Colijn, and Brian Kemmenoe at OSU for XRD and TEM assistance.

References and Notes

(1) Usuki, A.; Kawasumi, M.; Kojima, Y.; Okada, A.; Kurauchi, T.; Kamigaito, O. *J. Mater. Res.* **1993**, *8*, 1174.
(2) Usuki, A.; Kojima, Y.; Kawasumi, M.; Okada, A.; Fukushima, Y.; Kurauchi, T.; Kamigaito, O. *J. Mater. Res.* **1993**, *8*, 1180.
(3) Kojima, Y.; Usuki, A.; Kawasumi, M.; Okada, A.; Fukushima, Y.; Kurauchi, T.; Kamigaito, O. *J. Mater. Res.* **1993**, *8*, 1185.
(4) Pinnavaia, T. J.; Lan, T.; Wang, Z.; Shi, H.; Kaviratna, P. D. *ACS Symp. Ser.* **1996**, *622*, 250.
(5) Lan, T.; Pinnavaia, T. J. *Chem. Mater.* **1994**, *6*, 2216.
(6) Shi, H.; Lan, T.; Pinnavaia, T. J. *Chem. Mater.* **1996**, *8*, 1584.
(7) Wang, Z.; Pinnavaia; T. J. *Chem. Mater.* **1998**, *10*, 1820.
(8) Okada, A.; Usuki, A. *Mater. Sci. Eng.* **1995**, *C3*, 109.
(9) Messersmith, P.; Giannelis, E. P. *Chem. Mater.* **1994**, *6*, 1719.

(10) Gilman, J. W. *Appl. Clay Sci.* **1999**, *15*, 31.
(11) Dietsche, F.; Mülhaupt, R. *Polym. Bull.* **1999**, *43*, 395.
(12) Porter, D.; Metcalfe, E.; Thomas, M. J. K. *Fire Mater.* **2000**, *24*, 45.
(13) Gilman, J. W.; Jackson, C. L.; Morgan, A. B.; Harris, R.; Manias, E.; Giannelis, E. P.; Wuthenow, M. *Chem. Mater.* **2000**, *12*, 1866.
(14) Yano, K.; Kojima, Y.; Usuki, A.; Okada, A.; Kurauchi, T.; Kamigaito, O. *J. Polym. Sci., Part A: Polym. Chem.* **1993**, *31*, 2493.
(15) Lan, T.; Kaviratna, P. D.; Pinnavaia, T. J. *Chem. Mater.* **1994**, *6*, 573.
(16) Messersmith, P. B.; Giannelis, E. P. *J. Polym. Sci., Part A: Polym. Chem.* **1995**, *33*, 1047.
(17) Giannelis, E. P. *Adv. Mater.* **1996**, *8*, 29.
(18) Krishnamoorti, R.; Vaia, R. A.; Giannelis, E. P. *Chem. Mater.* **1996**, *8*, 1728.
(19) Vaia, R. A.; Giannelis, E. P. *Macromolecules* **1997**, *30*, 7990.
(20) Vaia, R. A.; Giannelis, E. P. *Macromolecules* **1997**, *30*, 8000.
(21) Balazs, A. C.; Singh, C.; Zhulina, E. *Macromolecules* **1998**, *31*, 8370.
(22) Ginzburg, V. V.; Balazs, A. C. *Macromolecules* **1999**, *32*, 5681.
(23) Ginzburg, V. V.; Singh, C.; Balazs, C. *Macromolecules* **2000**, *33*, 1089.
(24) Lan, T.; Kaviratna, P. D.; Pinnavaia, T. J. *Chem. Mater.* **1995**, *7*, 2144.
(25) Brown, J. M.; Curliss, D.; Vaia, R. A. *Chem. Mater.* **2000**, *12*, 3370.
(26) Wang, M. S.; Pinnavaia, T. J. *Chem. Mater.* **1994**, *6*, 468.
(27) Flory, P. J. *Principle of Polymer Chemistry*; Cornell University Press: New York, 1967.
(28) Noh, M. W.; Lee, D. C. *Polym. Bull.* **1999**, *42*, 619.
(29) Lee, D. C.; Jang, L. W. *J. Appl. Polym. Sci.* **1996**, *61*, 1117.
(30) Okamoto, M.; Moritaa, S.; Taguchi, H.; Kim, Y. H.; Kataka, T.; Tateyama, H. *Polymer* **2000**, *41*, 3887.
(31) Biasci, L.; Alietto, M.; Ruggeri, G.; Ciardelli, F. *Polymer* **1994**, *35*, 3296.
(32) Doh, J. G.; Cho, I. *Polym. Bull.* **1998**, *41*, 511.
(33) Dietsche, F.; Thomann, Y.; Thomann, R.; Mülhaupt, T. *J. Appl. Polym. Sci.* **2000**, *75*, 396.
(34) Weimer, M. W.; Chen, H.; Giannelis, E. P.; Sogah, D. Y. *J. Am. Chem. Soc.* **1999**, *121*, 1615.
(35) Huang, X.; Brittain, W. J. *Polym. Prepr.* (*Am. Chem. Soc., Div. Polym. Chem.)* **2000**, *41*, 521.
(36) Bandyopadhyay, S.; Giannelis, E. P.; Hsieh, A. J. *Polym. Mater. Sci. Eng.* **2000**, *82*, 208.
(37) Brindley, G. W.; Brown, G. *Crystal Structures of Clay Minerals and Their X-ray Identification*; Mineralogical Society: London, 1980.
(38) Moore, D. M.; Reynolds, R. C. *X-ray Diffraction and the Identification and Analysis of Clay Minerals*; Oxford University Press: New York, 1989.
(39) Theng, B. K. *The Chemistry of Clay-Organic Reactions*; John Wiley & Sons: New York, 1974.
(40) Blumstein, A. *J. Polym. Sci., Part A* **1965**, *3*, 2653.
(41) Solomon, D. H.; Rosser, M. J. *J. Appl. Polym. Sci.* **1965**, *9*, 1261. Solomon, D. H.; Loft, B. C. *J. Appl. Polym. Sci.* **1968**, *12*, 1253.
(42) Slabaugh, W. H.; St. Clair, A. D. *J. Colloid Interface Sci.* **1969**, *29*, 586.
(43) Cody, C. A.; Reichert, W. W. *NLGI Spokesman* **1986**, *49*, 437.
(44) Magauran, E. D.; Kieke, M. D.; Reichert, W. W.; Chiavoni, A. *NLGI Spokesman* **1987**, *50*, 453.
(45) Fu, X.; Qutubuddin, S. *Polymer* **2001**, *42*, 807.
(46) Vaia, R. A.; Jandt, K. D.; Kramer, E. J.; Giannelis, E. P. *Macromolecules* **1995**, *28*, 8080.
(47) Vaia, R. A.; Jandt, K. D.; Kramer, E. J.; Giannelis, E. P. *Chem. Mater.* **1996**, *8*, 2628.
(48) Krishnamoorti, R.; Giannelis, E. P. *Macromolecules* **1997**, *30*, 4097.
(49) Ren, J.; Silva, A. A. S.; Krishnamoorti, R. *Macromolecules* **2000**, *33*, 3739.
(50) Cho, J. W.; Paul, D. R. *Polymer* **2001**, *42*, 1083.
(51) Olphen, H. v. *An Introduction to Clay Colloid Chemistry*; John Wiley & Sons: New York, 1963.

MA010061X